Inorganic Chemistry

Article

pubs.acs.org/IC

A Strong Metal-to-Metal Interaction in an Edge-Sharing Bioctahedral Compound that Leads to a Very Short Tungsten−Tungsten Double Bond

Gina M. Chiarella,[†] F. Albert Cotton,[§] Carlos A. Murillo,*[,†] and Qinliang Zhao*[,‡]

[†]Department of Chemistry, Texas A&M University, P.O. Box 30012, College Station, Texas 77842-3012

[‡]Department of Chemistry, University of the Pacific, 3601 Pacific Avenue, Stockton, CA 95211

Supporting Information

ABSTRACT: An ionic edge-sharing bioctahedral (ESBO) species has been prepared having a tetramethylated bicyclic guanidinate with two fused six-membered rings characterized by a fairly flat N−C(N)−N skeleton and abbreviated as TMhpp. The anion has two W^{IV} atoms bridged by two oxo groups; the metal atoms are also spanned by two bridging guanidinate ligands, and each has two monodentate chlorine atoms. The complex formulated as $(H_2TMhpp)_2[W(\mu\text{-}O)(\mu\text{-}TMhpp)Cl_2]_2$ has the shortest W−W distance (2.3318(8) Å) of any species with a $\sigma^2\pi^2$ electronic configuration. The anion and cations are connected by hydrogen bonds. To unambiguously ascertain the existence of the double-bonded $W_2(\mu\text{-}O)_2$ entity, density functional theory calculations and natural bond orbital analyses were done on an analogous but hypothetical species with a $W_2(\mu\text{-}OH)_2$ core having trivalent tungsten atoms and a possible $\sigma^2\pi^2\delta^2$ electronic configuration. The calculations decidedly support the presence of tungsten−oxo instead of tungsten−hydroxo groups and thus the existence of the double-bonded $W_2(\mu\text{-}O)_2$ core. The strong bonding interaction between metal atoms is a clear indication that under certain circumstances the two octahedra in ESBO species do not behave as the sum of two mononuclear compounds.

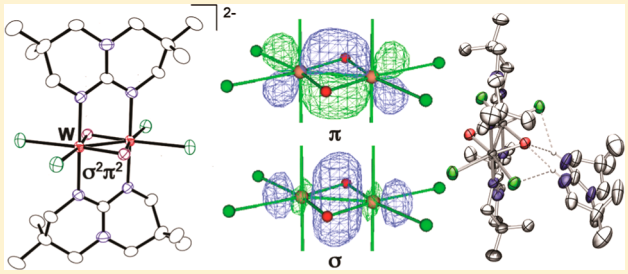

INTRODUCTION

An octahedron having a positively charged central metal atom surrounded by six electron-donor ligands is without a doubt one of the most iconic geometric structures encountered in inorganic chemistry.[1] Such an image is ubiquitous not only for mononuclear species but also in instances of increasing complexity where two such entities aggregate to form bioctahedral compounds that share either an edge or a face, that is, edge-sharing bioctahedral (ESBO, **I**) compounds or face-sharing bioctahedral (FSBO, **II**) complexes, as shown in Scheme 1. The level of complexity may increase as more units share vertices and edges such as those found in close packing of anions in salts.

A question that frequently comes up while teaching an inorganic chemistry course is whether in the study of species with multiple octahedra the chemical behavior of the metal centers closely resembles the sum of individual species, or whether there is some type of synergy, and if so what is the effect? In this manuscript we will explore a case in which the positively charged metal centers strongly interact with each other, forming an uncharacteristically strong metal−metal bond as implied by an exceptionally short intermetallic separation of 2.3318(8) Å for an ESBO compound (**1**) having two d^2-tetravalent tungsten atoms and a $[W^{IV}(\mu\text{-}O)(\mu\text{-}LL)Cl_2]_2^{2-}$ core, where LL is the mononegative, bridging, bicyclic guanidinate ligand TMhpp prepared by deprotonation of HTMhpp, (**III** in Scheme 1).[2,3]

For a general survey of metal−metal bonding in ESBO compounds, the reader is referred to an inorganic chemistry textbook.[4] There are also relevant calculations reported for compounds of the type $M_2X_6L_2$ (M = trivalent transition metal atom, X = halide, L = phosphine) for species with d^1−d^1 to d^5−d^5 electronic configurations[5] as well as an analysis of the electronic structure of such complexes.[6] Briefly, as it is shown in Figure 1 for an ESBO compound, single (σ^2) or double ($\sigma^2\pi^2$) bonds may form by overlap of pairs of d orbitals from the metal centers having d^1 and d^2 electronic configurations, respectively. Species with two metal atoms with d^4 electronic configurations may also have a formal bond order of 2 because the δ and δ^* orbitals will be filled. A more complex situation usually presents itself for species with metal centers with a d^3 configuration

Scheme 1

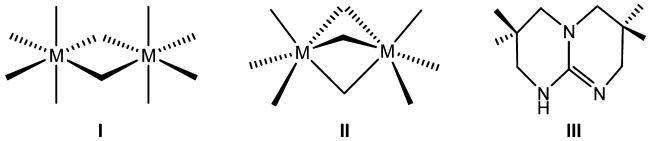

I II III

Received: December 4, 2013
Published: January 31, 2014

   dx.doi.org/10.1021/ic402992n | *Inorg. Chem.* 2014, 53, 2288−2295

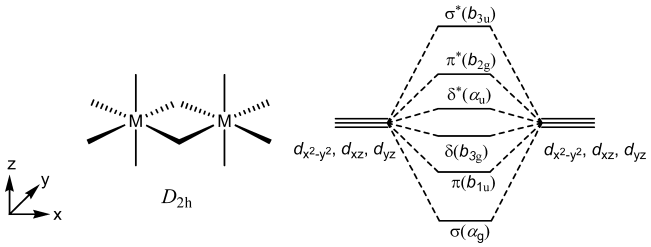

Figure 1. A representation of the molecular orbital diagram for ESBO species in which three direct d−d overlaps are possible. Frequently bonding δ, antibonding δ^*, and antibonding π^* levels (b_{3g}, α_u, b_{2g}) are similar in energy, and quite often their order in energy changes from that shown in the diagram. Note that in the Cartesian coordinate system in the inset, d_{xy} and d_{z^2} orbitals are used for metal-to-ligand bonding.

where one could visualize a triple bond of the type $\sigma^2\pi^2\delta^2$. Because there is often an energy inversion between the δ orbital and the δ^* orbital caused by the interactions with ligand orbitals in most cases there is a formal bond order of less than three.

It is important to note that ESBO and FSBO compounds of the type $M_2X_6L_n$, n = 3 or 4, are a dominant feature in the chemistry of trivalent molybdenum and tungsten (d^3 systems).[7] The metal−metal separations are often around 2.4−2.7 Å. For example, the W−W distance is 2.6726(8) Å in the ESBO compound 1,2,5,6-$[W(\mu\text{-Cl})(\eta^2\text{-dmpe})Cl_2]_2$,[8] dmpe = bis-(dimethylphosphino)ethane, 2.7113(8) and 2.7397(7) Å in ESBO $[W(\mu\text{-Cl})Cl_2(PR_3)_2]_2$ but a bit shorter (2.438(2) Å) in FSBO $(HPEt_3)[W_2Cl_7(PEt_3)_2]$.[9] When the oxidation state increases as in $W^{IV}{}_2Cl_4(\mu\text{-OR})_2(OR)_2(ROH)_2$ (R = Me, Et), the W−W distances of 2.481(1) and 2.483(1) Å are also relatively short. In this compound, the $W-OR_{bridge}$ distances are 2.034(6) and 2.022(8) Å, and theoretical calculations were consistent with a $\sigma^2\pi^2$ electronic configuration.[10] A similar W−W distance of 2.4791(7) Å was found in a complex having a W_2^{7+} core, namely $W_2(\mu\text{-H})(\mu\text{-OEt})(\mu\text{-}O_2CC_6H_5)(\eta^1\text{-OEt})_2Cl_2(\eta^2\text{-}P,P'\text{-dppp})$, dppp = bis(diphenylphosphino)-propane.[11]

As far as the ligand in **1** is concerned, it should be noted that guanidinate ligands characterized by their fairly flat N−C(N)−N skeleton have become increasingly important in coordination chemistry, and their anions have been used to stabilize a series of mononuclear as well as dinuclear species.[12] These and some parent guanidine compounds have also been used in catalytic processes.[13] A particularly relevant aspect of the bicyclic guanidinate ligands is their ability to stabilize unusually high oxidation states in dinuclear paddlewheel compounds.[14] Some examples are those with Cr_2^{5+},[15] Mo_2^{6+},[16] W_2^{6+},[17] Re_2^{7+},[18] Os_2^{7+},[19] Re_2^{8+},[20] Ir_2^{6+},[21] Rh_2^{5+},[22] and Pd_2^{6+} units.[23] Because of the extraordinary ability of the bicyclic guanidinate ligands to stabilize metal atoms in high oxidation states, the reduced species can act as strong reducing agents. In particular the family of compounds $W_2(hpp)_4$,[3,17,24] $W_2(TMhpp)_4$, and $W_2(TEhpp)_4$ possesses the lowest ionization energy of any stable closed-shell species.[25] This effect has been attributed to the strong interaction of the electrons in the δ orbitals of the quadruple-bonded W_2^{4+} species and the electrons in the π orbitals of the bicyclic guanidinate ligand.[17b]

Here we report the synthesis, structural characterization, density function theory (DFT) studies and natural bond orbital (NBO) analyses of a species having a W_2^{8+} core and the formula $(H_2TMhpp)_2[W(\mu\text{-O})(\mu\text{-TMhpp})Cl_2]_2$ (**1**, Scheme 2). The anion represents the ESBO species with the shortest

Scheme 2

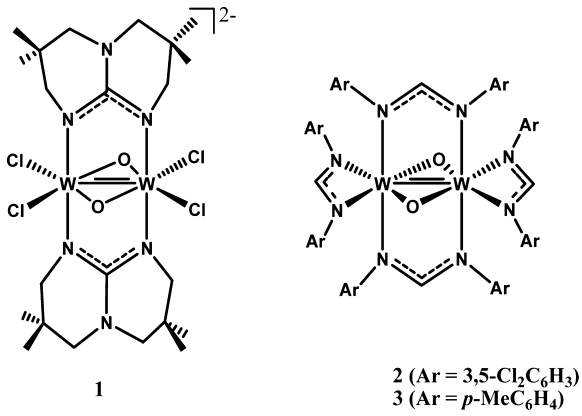

1

2 (Ar = 3,5-$Cl_2C_6H_3$)
3 (Ar = *p*-MeC_6H_4)

known W−W separation (2.3318(8) Å). This distance is about 0.10 Å shorter than the corresponding ones in analogous compounds with a bond order of 2 having a $\sigma^2\pi^2$−electronic configuration.[10] Evidence from DFT calculations indicates that the two formamidinate compounds **2** and **3** in Scheme 2, reported to have $W_2(\mu\text{-OH})_2$ cores,[26,27] most likely contain $W_2(\mu\text{-O})_2$ units.

RESULTS AND DISCUSSION

Syntheses. Reaction of $W(CO)_6$ with neutral bicyclic guanidinate ligands such as Hhpp is known to proceed in *o*-dichorobenzene through a series of steps that eventually lead to $W_2(hpp)_4Cl_2$. This compound serves as an easily made, stable precursor for one of the most easily ionized molecules, namely, $W_2(hpp)_4$. By controlling the reaction temperature various intermediate compounds have been isolated.[17b,24] The processes for which products have been characterized are shown in eqs Eq 1−Eq 3.

$$W(CO)_6 + 2Hhpp \rightarrow W(CO)_4(Hhpp)_2 + 2CO \quad \text{(Eq 1)}$$

$$2W(CO)_4(Hhpp)_2 \rightarrow (\eta^2\text{-hpp})W(\mu\text{-CO})_2(\mu\text{-hpp})_2W(\eta^2\text{-hpp}) + 2H_2 + 6CO \quad \text{(Eq 2)}$$

$$W_2(\mu\text{-CO})_2(hpp)_4 + 2(o\text{-dichlorobenzene}) \rightarrow W_2(\mu\text{-hpp})_4Cl_2 + 2CO + C_{12}H_8Cl_2 \quad \text{(Eq 3)}$$

For the preparation of **1**, oxidation accompanied by partial hydrolysis of $W_2(\mu\text{-TMhpp})_4Cl_2$ was carried out serendipitously early on but intentionally later on. For this purpose it was unnecessary to isolate the triply bonded paddlewheel compound $W_2(\mu\text{-TMhpp})_4Cl_2$.[28] The overall process is summarized in eq Eq 4.

$$W_2(\mu\text{-TMhpp})_4Cl_2 + 1/2O_2 + 2HCl + H_2O \rightarrow (H_2TMhpp)_2[W(\mu\text{-O})(\mu\text{-TMhpp})Cl_2]_2 \quad \text{(Eq 4)}$$

Structure. The solid-state structure of the anion in the ESBO species **1**·$2CH_2Cl_2$ is shown in Figure 2. Each of the d^2 tungsten atoms has a formal oxidation state of 4 and thus a formal W_2^{8+} unit and a $\sigma^2\pi^2$ electronic configuration. The

dx.doi.org/10.1021/ic402992n | Inorg. Chem. 2014, 53, 2288−2295

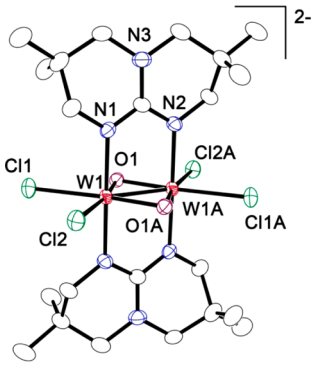

Figure 2. Solid-state structure of the dianion in $1{\cdot}2CH_2Cl_2$ showing the edge-sharing bioctahedral (ESBO) core arrangement. Because of a crystallographically imposed inversion center only one-half of the anion is crystallographically independent. W–W = 2.3318(8) Å, W–Cl = 2.499(2) and 2.504(2) Å, W–*N* = 2.095(6) Å, $W-O_{bridge}$ = 1.962(5) and 1.963(5) Å.

dianion in **1** has two oxygen atoms that serve as bridges between the tungsten atoms generating a $W_2(\mu\text{-}O)_2^{4+}$ core. The two TMhpp ligands also span the dimetal unit, and two terminal chlorine atoms per metal atom complete the metal atom coordination sphere. The two cations are formally the protonated parent guanidine, H_2TMhpp. The W–W distance in the anion of 2.3318(8) Å is by far the shortest distance reported in ESBO species having W_2^{8+} units (vide supra), which are typically >2.6 Å. The distance in **1** resembles that of 2.306[2] Å in a somewhat analogous Mo_2^{8+}/formamidinate compound, $Mo_2(\mu\text{-}O)_2(\mu\text{-DXylF})_2(\eta^2\text{-acetate})_2$, DXylF = di-3,5-xylylformamidinate.[29] This formamidinate compound has slightly unsymmetrical $Mo-O_{bridge}$ distances attributed to a Jahn–Teller effect, but such distortion is not detected in **1**, as observed in Table 1. DFT calculations have attributed the rhomboidal distortion to vibronic mixing of the ground electronic state and a low-lying $\pi\delta^*$ excited state.[30]

Table 1. Selected Bond Distances (Å) and Angles (deg) for Compounds 1–3

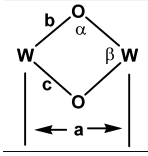

		1	2[26]	3[27]
a		2.3318(8)	2.3508(3)	2.3499(6)
b		1.962(5)	1.963(3)	1.947(3)
c		1.963(5)	1.972(3)	1.951(3)
α		72.9(2)	73.4(1)	74.1(1)
β		107.1(2)	106.6(1)	105.9(1)

Note that there are also two reports of compounds having the formula $(\eta^2\text{-formamidinate})W(\mu\text{-OH})_2(\mu\text{-formamidinate})_2W(\eta^2\text{-formamidinate})$ (**2** and **3**) where the formamidinate (RNC(H)NR) ligands are bis(3,5-dichlorophenyl)formamidinate (DClPhF)[26] and di-*p*-tolylformamidinate (DTolF).[27] Curiously, the reported W–W distances are 2.3508(3) Å and 2.3499(6) Å for the DClPhF and DTolF analogues, respectively, which are only 0.03 Å longer than that in **1** (Table 1). If indeed the bridging groups are hydroxide instead of oxide groups, the core would have a W_2^{6+} unit and possibly a $\sigma^2\pi^2\delta^2$ triple bond. But the similarity in the intermetallic distances and tungsten-to-oxygen distances generate some reservations on whether the assignment of **1** described thus far is correct.

In this context it is important to keep in mind that assignment of an OH versus an O group is generally impractical when X-ray crystallographic methods are used, especially in species with two heavy W atoms. Furthermore the absence of a signal for the OH groups in the ^{1}H NMR spectrum of **1** cannot be used as a definite proof that the bridging groups are oxygen atoms, since such signal may be obscured by other signals corresponding to a large number of hydrogen atoms in the guanidinate groups. In addition, one must also be careful with assignments of OH groups by ^{1}H NMR techniques, since signals for some of them appear close to where water from moist deuterated solvents would be expected. The highly symmetrical $1{\cdot}2CH_2Cl_2$ possesses a crystallographically imposed inversion center. Its structure has an additional and important probe over the formamidinate compounds to aid in the chemical assignment since there are hydrogen bonds linking the cations and anion. The crystallographically equivalent (but slightly disordered) cations directly interact using both of the N–H entities of the H_2TMhpp unit with both the chlorine and oxygen atoms of the ditungsten unit as shown in Figure 3 and Supporting Information, Figure S8. Clearly, this interaction would not be viable if the species described as being cationic were anionic or even neutral.

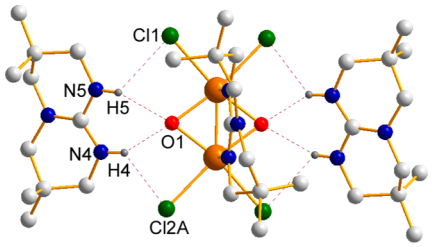

Figure 3. A view of how the crystallographically related cations and the anion strongly interact through hydrogen bonding shown as dashed lines. The TMhpp ligand below the plane of the paper was removed for clarity. Note that both of the N–H groups of the H_2TMhpp cation interact with the chlorine (green) and oxygen (red) atoms of the dianion. The distances of both crystallographically independent H bonds are 2.669(2) and 2.658(2) Å for Cl(1)···H(5) and Cl(2A)···H(4), respectively and 2.149(4) and 2.205(5) for O(1)···H(5) and O(1)···H(4), respectively. The corresponding distances between the N atoms (blue) and chlorine atoms are Cl(1)···N(5) = 3.24 Å and Cl(2A)···N(4) = 3.32 Å, while those between O and N atoms are O(1)···N(4) = 2.983 Å and O(1)···N(5) = 2.939 Å.

To further aid in the assignment, DFT calculations (vide infra) were pursued for species with the $W_2(\mu\text{-}O)_2$ core in **1** and an analogue with a hypothetical $W_2(\mu\text{-OH})_2$ core. However, before an account of the DFT calculations is provided, it is worth making some comparisons of the W–O distances in some known compounds having unambiguous assignments of $W_2(\mu\text{-}O)_2$ and $W_2(\mu\text{-OH})_2$ cores. Because of the larger negative charge in the oxo species relative to the hydroxo species, significantly shorter W–O distances are expected for the oxide relative to the hydroxide. In **1**, the $W-O_{bridge}$ distances are 1.962(5) and 1.963(5) Å, which are essentially the same as those reported for $W_2(\mu\text{-OH})_2(\mu\text{-DClPhF})_4(\eta^2\text{-DClPhF})_2$ (**2**, 1.963(3) and 1.972(3) Å)[26] and $W_2(\mu\text{-OH})_2(\mu\text{-DTolF})_4(\eta^2\text{-DTolF})_2$ (**3**, 1.947(3) and 1.951(3) Å).[27] These distances are also similar to those of 1.89(1) Å in a compound with a double bond and a W_2^{8+} core, $\{W_2(\mu\text{-}O)(\mu\text{-O}^t\text{Bu})(OSiMe_2{}^t\text{Bu})_5(py)_2\}$, in which the W–W distance is 2.488(1) Å.[31] By contrast in the hydroxo-containing compound

dx.doi.org/10.1021/ic402992n | Inorg. Chem. 2014, 53, 2288–2295

$[W_2(\mu\text{-}OH)_2L_2Br_2]Br_2$ (L = 1,4,7-diazacyclononane), which has trivalent tungsten atoms, the W−OH_{bridge} distance is over 0.10 Å longer (2.095(20) Å) than those in **1**. In this compound the W−W separation is 2.477(3) Å.[32] There is also a report of an unsymmetrical ESBO compound $W_2(\mu\text{-}O)(\mu\text{-}NC_6H_3Cl_2)(\mu\text{-}DClPhF)_2(\eta^2\text{-}DClPhF)_2$ having a W−W distance of 2.3972(9) Å and W−O distances of 1.956(8) and 1.964(7) Å.[33] Because this compound is diamagnetic, there is undoubtedly a W_2^{8+} unit that requires that the bridging group be O (not OH). Importantly these W−O bond distances are comparable to those in **1**. Similarly, for $K_3H[W_2(\mu\text{-}O)_2O_2F_6]$[34] the W−$O_{bridge}$ distances of 1.99(2) and 1.98(1) Å resemble those in **1**. In this compound the W−W separation is 2.620(1) Å. Another relevant comparison is provided by a pair of species containing two dimolybdenum units spanned by the formamidinate *N,N′*-(*m*-$CF_3C_6H_4$)NC(H)N(*m*-$CF_3C_6H_4$) abbreviated as D*m*CF_3F and linked by either two oxo or two hydroxo groups. For $Mo_2(Dm CF_3F)_3(\mu\text{-}OH)_2Mo_2(Dm CF_3F)_3$ the Mo−OH bond distance is 2.136(6) Å, while for the dioxo compound $Mo_2(Dm CF_3F)_3(\mu\text{-}O)_2Mo_2(Dm CF_3F)_3$ the corresponding Mo−O distances are significantly shorter (1.927(2) and 1.937(2) Å) but similar to those in **1**.[35] A comparable situation is observed in analogues containing the formamidinate ligand di(*p*-anisyl)formamidinate (DAniF).[36] In the latter, the reaction from the dihydroxo to the dioxo compound takes place in the crystal, and crystallographic measurements for both compounds were done on the same crystal. Therefore, it appears that the experimental evidence strongly supports the $W_2(\mu\text{-}O)_2$ formulation, but what do computations support?

DFT Studies. These calculations were carried out using a series of model compounds depicted in Figure 4. Importantly during all calculations no symmetry constraints were imposed. In all cases the RB3LYP function was used. The basis sets were either LANL2DZ for W with core potential, D95 for N, O, C, H; CC-PVDZ for Cl (basis set 1) or SDD for W with core potential, 6-311G** for N, O, C, H; CC-PVDZ for Cl (basis set 2). The dianion in **1** was modeled using the coordinates from the X-ray structure. For comparison, the dihydroxo dianion **1H** was also calculated as well as a neutral but hypothetical dioxo $W_2(\mu\text{-}O)_2(\mu\text{-}TMhpp)_2Cl_4$ species **1′** and a dihydroxo $W_2(\mu\text{-}OH)_2(\mu\text{-}TMhpp)_2Cl_4$ entity **1H′**.

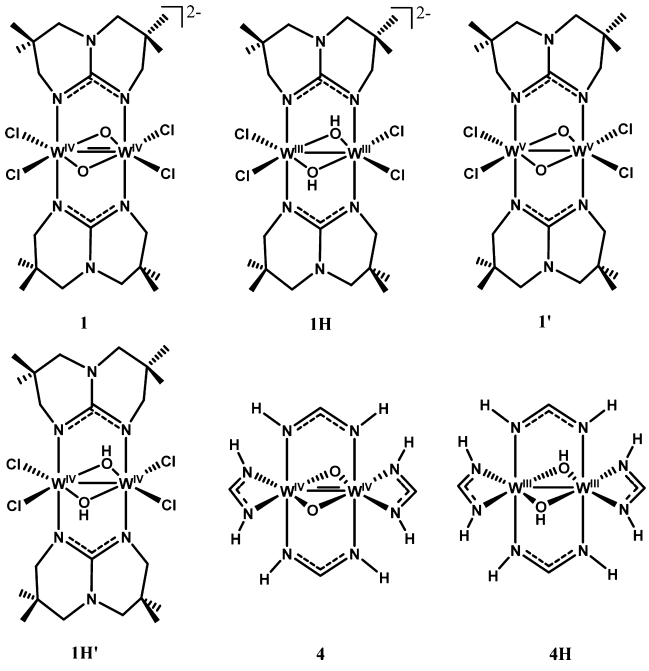

Figure 4. Model compounds used in DFT calculations.

Selected bond distances and angles from the calculations for the model dioxo dianion **1** and the model hydroxo **1H** are shown in Table 2. Additional computational data with details of the calculations are provided in the Supporting Information (vide infra). A quick inspection of Table 2 shows that the most sensitive parameters are the W−W and W−O distances. In both instances the computations reproduce quite well the observed distances found in the solid-state structure of **1**. The W−W_{exp} of 2.3318(8) Å is calculated as 2.361 and 2.360 Å with basis sets 1 and 2, respectively. This distance is almost 0.1 Å longer in the hydroxo model **1H**. Similarly, the calculated W−O distances of 1.990 and 1.980 Å for the dioxo anion model are only slightly longer than the W−O_{exp} of 1.962(5) and 1.963(5) Å, but those calculated for the corresponding hypothetical dihydroxo (**1H**) and the neutral dihydroxo (**1H′**) are significantly longer (2.120 and 2.040 Å, respectively).[37] Because the difference in W−O distances is clearly consistent with the change in oxidation state, the calculations strongly support the formulation of **1** as having a dianion with two W^{IV} atoms bridged by two oxo groups.

As noted above, there are reports of two formamidinate compounds having two W^{III} atoms and two bridging hydroxo groups but similar core distances to those in **1** (Table 1).[26,27] Because the similarities are so striking, DFT calculations were also done on the simplified formamidinate model compounds shown in Figure 4 with either two oxo (**4**) or two hydroxo groups (**4H**). In each case, the basis sets 1 and 2 were used; the results are given in Table S2 (see Supporting Information). Again, the computations clearly favor the existence of oxo over hydroxo groups. The experimental W−W distance in the compound purported to be $[W(\mu\text{-}OH)(\mu\text{-}DTolF)(\eta^2\text{-}DTolF)]_2$ is 2.3499(6) Å. The calculated distance of 2.385 Å

Table 2. Selected Bond Distances (Å) and Angles (deg) for 1, $(H_2TMhpp)_2[W(\mu\text{-}O)(\mu\text{-}TMhpp)Cl_2]_2$ and 1H, $[W(\mu\text{-}OH)(\mu\text{-}TMhpp)Cl_2]_2^{2-}$[a]

		calc for **1**		calc for **1H**
	exp	basis set 1	basis set 2	basis set 1
W1−W2	2.3318(8)	2.361	2.360	2.425
W1−Cl1	2.504(2)	2.620	2.590	2.580
W1−Cl2	2.499(2)	2.600	2.610	2.590
W1−N1	2.095(6)	2.110	2.140	2.090
W1A−N2	2.095(6)	2.110	2.140	2.090
W1−O1	1.962(5)	1.990	1.990	2.120
W1−O1A	1.963(5)	1.980	1.980	2.120
Cl1−W1−W2	137.46(5)	138.13	137.76	136.22
Cl2−W2−W1	136.10(5)	138.16	137.97	136.40
W1−O1−W1A	72.9(2)	72.76	72.93	69.64
O1−W1−O1A	107.1(2)	107.43	107.13	110.35
O1−W1−Cl1	83.9(2)	84.58	84.43	81.17
Cl1−W1−Cl2	86.44(6)	83.69	84.25	87.37
N1−C1−N2	118.6(7)	119.27	119.88	118.82
N4−C12−N5 (from countercation)	120.9(8)			

[a]For a complete set of distances and angles for **1H** using basis sets 1 and 2, see Supporting Information.

dx.doi.org/10.1021/ic402992n | *Inorg. Chem.* 2014, 53, 2288−2295

for the dioxo model (**4**) is only slightly longer than the experimental value, but it is significantly longer (2.450 Å) for the dihydroxo model (**4H**). More importantly, the average experimental W−O_{bridge} distance of 1.949[4] Å resembles more closely that in the dioxo model (2.000 and 1.999 Å for the basis sets 1 and 2, respectively) than it does for the dihydroxo model (2.130 and 2.140 Å, for the basis sets 1 and 2, respectively). These results strongly support the existence of a $W_2(\mu\text{-O})_2$ core instead of a $W_2(\mu\text{-OH})_2$ core in these formamidinate compounds.

The calculations for the model of the anion in **1** also show that the HOMO corresponds to a π interaction between d orbitals from the metal atoms and π^* interaction to the oxygen and chlorine lone pairs while the HOMO−1 is a σ interaction between d orbitals from the metal atoms. In the latter, there is also a σ^* interaction to the O lone pairs and a π^* interaction to the Cl lone pairs that is pictorially shown in Figure 5.[38] Importantly these interactions between the metal-based σ and π orbitals and ligand lone pairs are not insignificant even though they do not affect the calculated W−W bond order of 2 and the electronic configuration of $\sigma^2\pi^2$ since all bonding and antibonding orbitals are filled, as shown in the molecular orbital (MO) interaction diagram in Supporting Information, Figure S3. In addition, Figure 5 also shows that the δ bond between the two tungsten centers has been raised to a higher energy level than the δ^* bond because of the strong π^* interactions to the oxygen lone pairs. The energy inversion of the delta bond (antibonding and bonding) is consistent with early studied ESBO compounds[5,6] and more recent findings in a dimolybdenum analogue.[30]

For the dioxo-formamidinate model **4** the bonding MOs resemble those in **1**. The HOMO is a metal-based π orbital formed by overlap of two tungsten d orbitals while the HOMO−1 is a metal-based σ orbital derived by overlap of two W d orbitals.[39] This gives again a ground state $\sigma^2\pi^2$ electronic configuration. The LUMO+1 is similar to that of **1**; however, the LUMO significantly differs from that of **1**. In the dioxo-formamidinate model **4**, the LUMO is a metal-based π^* orbital formed by overlap between two W d orbitals with strong π interaction to the formamidinate p orbitals. In a comparison of the orbital energy ordering of metal-based orbitals between the model anion **1** and model complex **4**, it is evident that the strong bonding interaction between the p orbitals from the two formamidinates in the axial positions and metal d orbitals in **4** significantly lowers the energy of the metal-based π^* orbital formed between the two tungsten centers. Because the difference occurs in unoccupied antibonding orbitals, there are no implications on the ground state, and this is why the experimental W−W bond distances in **1**, **2**, and **3** are so similar.

To further probe the bond character between the two W atoms in the ESBO compounds, NBO analyses were carried out using geometry-optimized models **1** and **4**. Consistent with the formal double bond formulation between the two metal atoms the results from these computations depicted in Figure 6 show a σ bond between two $d_{x^2-y^2}$ orbitals from W atoms and π interactions between the two d_{xz} orbitals. A bond-order analysis using Wiberg bond indexes from the NBO analysis (Supporting Information, Figures 6S and 7S) produced an effective W−W bond order of 1.61 for **1** and 1.55 for **4** using basis set 1, and 1.70 for **1** and 1.65 for **4** using basis set 2. This is consistent with the postulated formal double bond character.[40] These Wiberg bond index values are consistent with the slightly shorter experimentally observed bond distance in **1** than those in **2** and **3** (W−W: 2.3318(8) Å in **1**, 2.3508(3) Å in **2**, 2.3499(6) Å in **3**).

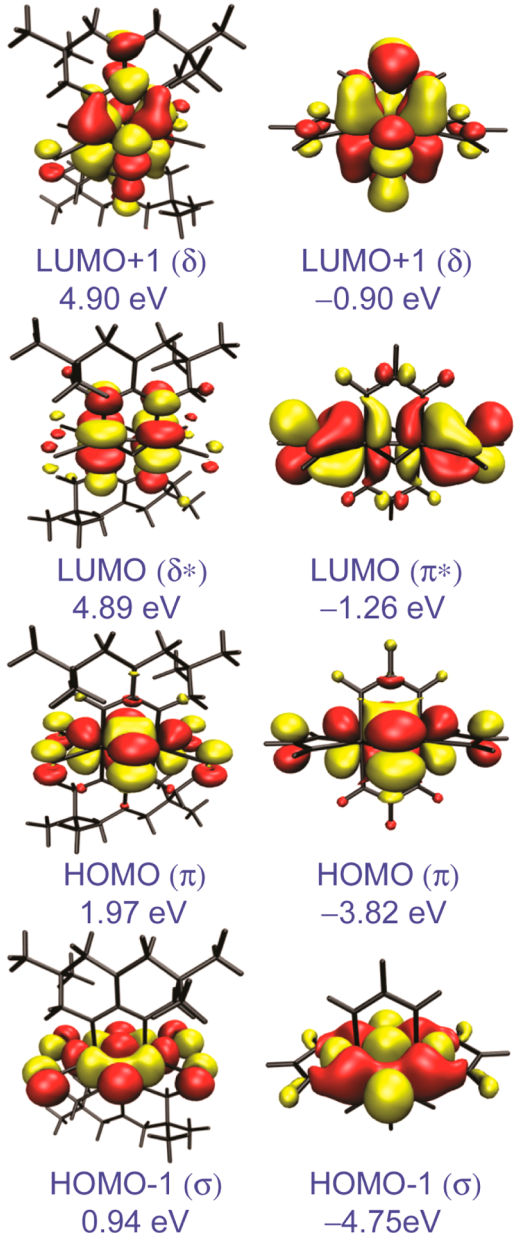

Figure 5. Selected MO diagrams with 0.02 contour surface for the model anion $[W(\mu\text{-O})(\mu\text{-TMhpp})Cl_2]_2^{2-}$ in **1** (left) and model compound **4** $W_2(\mu\text{-O})_2(\mu\text{-HNC(H)NH})_2(\eta^2\text{-HNC(H)NH})_2$ (right), derived from calculations using the basis set 1. Both sets of calculations are consistent with a $\sigma^2\pi^2$ electronic configuration, but there are differences in the unoccupied LUMO orbitals.

CONCLUDING REMARKS

An anion having a $W_2(\mu\text{-O})_2$ core with two tetravalent metal centers has been structurally characterized, and an unambiguous chemical assignment has been made with support from the hydrogen bonding pattern, DFT, and NBO analyses. The ditungsten species has a $\sigma^2\pi^2$ electronic configuration and a double bond between metal atoms. DFT calculations strongly support the dioxo formulation over that having dihydroxo groups. The ESBO compound $(H_2TMhpp)_2[W(\mu\text{-O})(\mu\text{-TMhpp})Cl_2]_2$ (**1**) has a very short W−W bond distance of

dx.doi.org/10.1021/ic402992n | Inorg. Chem. 2014, 53, 2288−2295

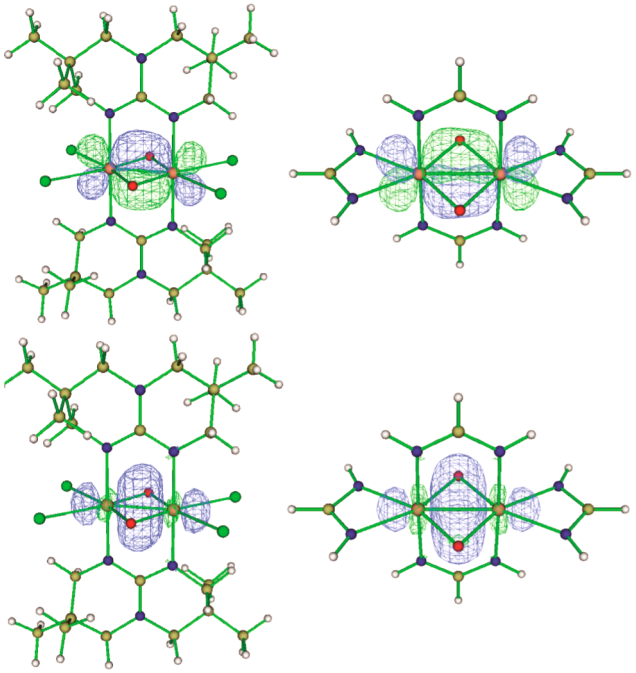

Figure 6. The two bonding orbitals between the W atoms with 0.05 contour surface for the $[W(\mu\text{-}O)(\mu\text{-}TMhpp)Cl_2]_2^{2-}$ anion in **1** (left) and the model $W_2(\mu\text{-}O)_2(\mu\text{-}NHC(H)NH)_2(\eta^2\text{-}NHC(H)NH)_2$ (**4**, right), derived from NBO analysis using the basis set 1. The σ bond between two $d_{x^2-y^2}$ orbitals is represented by the lower pair, while the π interaction between d_{xz} orbitals is depicted above.

2.3318(8) Å and short W−O_{bridge} distances of 1.962(5) and 1.963(5) Å. With support from theoretical calculations and similarity of bond distances with those of published formamidinate compounds purported to have $W_2(\mu\text{-}OH)_2$ cores and formulas $[W(\mu\text{-}OH)(\mu\text{-formamidinate})(\eta^2\text{-formamidinate})]_2$,[26,27] it is proposed that these compounds be reformulated as dioxo instead of dihydroxo species.

EXPERIMENTAL SECTION

General Procedures. Procedures were performed under a nitrogen atmosphere unless otherwise noted. The Schlenk line was equipped with a mercury bubbler to allow an increase of internal pressure.[41] Hexanes, *o*-dichlorobenzene, and dichloromethane were purchased from Aldrich. With the exception of *o*-dichlorobenzene, the solvents were purified using a Glass Contour solvent system. $W(CO)_6$ was obtained from commercial sources, and HTMhpp was prepared as previously described.[2]

Physical Characterization. ^{1}H NMR spectra were recorded on a Unity Plus 300 NMR spectrometer, using solvent peaks to reference chemical shifts (δ). Elemental analysis was performed by Robertson Microlit Laboratories, Inc., Madison, NJ, USA.

Synthesis of $(H_2TMhpp)_2[W(\mu\text{-}O)(\mu\text{-}TMhpp)Cl_2]_2$, 1. A mixture of 0.240 g (0.682 mmol) of $W(CO)_6$ and 0.300 g (1.53 mmol) of HTMhpp was placed in a 100 mL-Schlenk flask equipped with a stir bar, and the flask was filled with nitrogen. An aliquot of 15 mL of nondried *o*-dichlorobenzene was then added, and the flask was fitted with a water-cooled coldfinger. The pale yellow reaction mixture was heated to 200 °C under nitrogen for 5 h.[41] During the reflux period, the color of the reaction mixture changed to green. The reaction mixture was cooled to near room temperature and was briefly exposed to air, and the mixture was heated again under nitrogen to 200 °C for 5 min. The reaction mixture was cooled, filtered, and the solvent removed under vacuum. The green solid was dissolved in 10 mL of methylene chloride contained in a Schlenk tube and layered with hexanes. After 10 d green, block-shaped crystals of $\mathbf{1}\cdot 2CH_2Cl_2$ suitable for X-ray diffraction were obtained. Yield 0.351 g, 78%. Anal. Calcd for $W_2C_{44}H_{84}Cl_4N_{12}O_2$ (**1**): C, 39.95; H, 6.40; N, 12.71%. Found: C, 40.17; H, 6.24; N, 12.49%. ^{1}H NMR in $CDCl_3$ ppm: 3.052 (s), 2.911 (s), 1.052 (s).

X-ray Structure Determination. A crystal of $\mathbf{1}\cdot 2CH_2Cl_2$ was coated with Paratone oil and mounted on a nylon Cryoloop affixed to a goniometer head. Data were collected on a Bruker SMART 1000 CCD area detector system using omega scans of 0.3 deg/frame, with exposure of 30 s/frame at 213 K. Refinement was carried out in the orthorhombic space group *Pbca* having four molecules in the unit cell. Cell parameters were determined using the SMART software suite.[42] Data reduction and integration were performed with the software SAINT.[43] Absorption corrections were applied using the program SADABS.[44] The positions of the metal atoms were found via direct methods using the program SHELXTL.[45] Subsequent cycles of least-squares refinement followed by difference Fourier syntheses revealed the positions of the remaining non-hydrogen atoms. Hydrogen atoms were added in idealized positions. The anion is centered on a crystallographically imposed inversion center. The symmetry-related H_2TMhpp cations were disordered, as is often the case with bicyclic guanidinate-type species that form an envelope-type structure.[46] Specifically, there was disorder on the nitrogen, methylene, and methyl groups attached to one of the quaternary carbon atoms. The disorder was treated using an additional free variable. This resulted in two site-occupancy factors with a major component of 61.63% and a minor component of 38.37%. All non-hydrogen atoms were refined with anisotropic displacement parameters. All hydrogen atoms were included in the calculation of the structure factors. Data collection and refinement parameters are summarized in Table 3, and selected bond distances and angles are listed in Tables 1 and 2.

Table 3. Selected Crystallographic Data

compound	$\mathbf{1}\cdot 2CH_2Cl_2$
chemical formula	$C_{46}H_{88}Cl_8N_{12}O_2W_2$
fw	1492.58
space group	*Pbca*
a (Å)	17.952(7)
b (Å)	19.560(7)
c (Å)	17.598(7)
V (Å^3)	6179(4)
Z	4
d_{calcd} (g cm^{-3})	1.604
μ (mm^{-1})	4.111
T (K)	213
$R1^a$ (w$R2$)^b	0.0473 (0.1088)

$^a R1 = [\sum w(F_o-F_c)^2/\sum wF_o^2]^{1/2}$. ^{b}w$R2 = [\sum[w(F_o^2-F_c^2)^2]/\sum w(F_o^2)^2]^{1/2}$, $w = 1/[\sigma^2(F_o^2) + (aP)^2 + bP]$, where $P = [\max(F_o^2,0) + 2(F_c^2)]/3$.

Computational Details. DFT[47] calculations were performed with the hybrid Becke 3-parameter exchange functional[48] and the Lee−Yang−Parr nonlocal correlation functional[49] (B3LYP) implemented in the Gaussian 03 (Revision C.02) program suite.[50] To allow for comparisons, all model compounds were computed using two independent basis sets. The first basis set 1 used double-ζ basis set (LANL2DZ) for W with a small effective core potential (ECP) representing the 1s2s2p3s3p3d core,[51] double-ζ quality basis sets (D95) for N, O, C, H,[52] as well as correlation consistent double-ζ basis sets (CC-PVDZ) for Cl.[53] The second basis set 2 used SDD for W with an effective core potential of 6-311g** for N, O, C, and H and CC-PVDZ for Cl.[40] Calculations were carried out without symmetry constraints using the model compounds depicted in Figure 4. Geometry optimizations of the model anion $[W_2(\mu\text{-}O)_2(\mu\text{-}TMhpp)_2Cl_4]^{2-}$ in **1** were done using the parameters from the crystal structure as starting points. The model compound **4**, $W_2(\mu\text{-}O)_2(\mu\text{-}HNC(H)NH)_2(\eta^2\text{-}HNC(H)NH)_2$, was simplified relative to that in the crystal structure by replacing the *p*-tolyl groups in **3** with hydrogen

dx.doi.org/10.1021/ic402992n | Inorg. Chem. 2014, 53, 2288−2295

atoms.[27] The models **1H**, **1′**, and **1H′** were directly derived from the structure of **1** by adding hydrogen atoms to the oxo bridges or by removing electrons for the corresponding anion, while **4H** was modified from **4** by adding hydrogen atoms to the oxo bridges. Selected MOs for models **1** and **4** are in Figure 5 as well as Figures S1 and S2 in the Supporting Information. MO interaction diagrams in models **1** and **4** are shown in Supporting Information, Figures S3 and S4. The general agreement between the calculated and the experimental geometric data shown in Table 2, Supporting Information, Tables S1 and S2 suggests that such a simplification is reasonable and appropriate. NBO analysis was performed by using the method built in the Gaussian 03 program.[50] Selected bonding and antibonding orbitals between W atoms and bond-order analysis for the geometry-optimized models **1** and **4** from NBO analysis are in Figure 6 and in Supporting Information, Figures 5S–7S. All computations were carried out on a Dirac SGI Altix 350 32-processor computer located at the University of the Pacific.

■ ASSOCIATED CONTENT

Supporting Information

Tables of calculated bond distances and angles for the models **1H**, **1′**, **1H′** as well as **4** and **4H**, tables of electron density distribution, selected MO diagrams, additional comments on metal–ligand orbital interactions, MO interaction diagrams, orbitals, and Wiberg bond indexes from NBO analysis, and a figure showing the H-bonding in **1** in pdf. X-ray crystallographic data for **1**·2CH_2Cl_2 in standard CIF format. This material is available free of charge via the Internet at http://pubs.acs.org.

■ AUTHOR INFORMATION

Corresponding Author

*E-mail: murillo@tamu.edu (C.A.M.), qzhao@pacific.edu (Q.Z.).

Notes

The authors declare no competing financial interest.

■ ACKNOWLEDGMENTS

This work was supported by the Robert A. Welch Foundation and Texas A&M University. C.A.M. also thanks the National Science Foundation (IR/D support). Q.Z. is grateful to the Department of Chemistry at University of the Pacific for financial support.

■ REFERENCES

(1) Cotton, F. A.; Wilkinson, G.; Murillo, C. A.; Bochmann, M. *Advanced Inorganic Chemistry*, 6th ed., John Wiley & Sons, Inc.: New York, 1999.

(2) Chiarella, G. M.; Cotton, F. A.; Ibragimov, S. A.; Murillo, C. A.; Wilkinson, C. C.; Young, M. D. *Polyhedron* **2012**, *58*, 7.

(3) TMhpp is the anion of 3,3,9,9-tetramethyl-1,5,7-triazabicyclo[4.4.0]dec-4-ene (HTMhpp), which is the tetramethylated analogue of the bicyclic guanidinate hpp (hpp = the anion of 1,3,4,6,7,8-hexahydro-2*H*-pyrimido[1,2-*a*]pyrimidine). For a discussion on the nomenclature, see: (a) Coles, M. P. *Chem. Commun.* **2009**, 3659. and references therein. (b) von Baeyer, A. *Ber. Dtsch. Chem. Ges.* **1900**, *33*, 3771. (c) Eckroth, D. R. *J. Org. Chem.* **1967**, *32*, 3362.

(4) For example, see ref 1, pages 647–652.

(5) Poli, R.; Torralba, R. C. *Inorg. Chim. Acta* **1993**, *212*, 123.

(6) Cotton, F. A. *Polyhedron* **1987**, *6*, 667.

(7) Kraatz, H.-B.; Boorman, P. M. *Coord. Chem. Rev.* **1995**, *143*, 35.

(8) Cotton, F. A.; Eglin, J. L.; James, C. A. *Inorg. Chem.* **1993**, *32*, 687.

(9) Barry, J. T.; Chacon, S. T.; Chisholm, M. H.; DiStasi, V. F.; Huffman, J. C.; Streib, W. E.; Van Der Sluys, W. *Inorg. Chem.* **1993**, *32*, 2322.

(10) Anderson, L. B.; Cotton, F. A.; DeMarco, D.; Fang, A.; Isley, W. H.; Kolthammer, B. W. S.; Walton, R. A. *J. Am. Chem. Soc.* **1981**, *103*, 5078.

(11) Carlson-Day, K. M.; Eglin, J. L.; Valente, E. J.; Zubkowski, J. D. *Inorg. Chim. Acta* **1999**, *284*, 300.

(12) (a) Foley, S. R.; Yap, G. P. A.; Richeson, D. S. *Polyhedron* **2002**, *21*, 619. (b) Soria, D. B.; Grundy, J.; Coles, M. P.; Hitchcock, P. B. *J. Organomet. Chem.* **2005**, *690*, 2315. (c) Coles, M. P.; Hitchcock, P. B. *Organometallics* **2003**, *22*, 5201. (d) Coles, M. P.; Hitchcock, P. B. *Dalton Trans.* **2001**, 1169. (e) Coles, M. P.; Hitchcock, P. B. *Inorg. Chim. Acta* **2004**, *357*, 4330. (f) Oakley, S. H.; Coles, M. P.; Hitchcock, P. B. *Inorg. Chem.* **2004**, *43*, 7564. (g) Coles, M. P.; Hitchcock, P. B. *Eur. J. Inorg. Chem.* **2004**, 2662. (h) Irwin, M. D.; Abdou, H. E.; Mohamed, A. A.; Fackler, J. P., Jr. *Chem. Commun.* **2003**, 2882. (i) Feil, F.; Harder, S. *Eur. J. Inorg. Chem.* **2005**, 4438. (j) Wilder, C. B.; Reitfort, L. L.; Abboud, K. A.; McElwee-White, L. *Inorg. Chem.* **2006**, *45*, 263. (k) Rische, D.; Baunemann, A.; Winter, M.; Fischer, R. A. *Inorg. Chem.* **2006**, *45*, 269. (l) Edelmann, F. T. *Chem. Soc. Rev.* **2009**, *38*, 2253. (m) Chiarella, G. M.; Melgarejo, D. Y.; Rozanski, A.; Hempte, P.; Perez, L. M.; Reber, C.; Fackler, J. P., Jr. *Chem. Commun.* **2010**, *46*, 136. (n) Lee, R.; Yang, Y. Y.; Tan, G. K.; Tan, C.-H.; Huang, K.-W. *Dalton Trans.* **2010**, *39*, 723. (o) Ciabanu, O.; Fuchs, A.; Reinmuth, M.; Lebkücher, A.; Kaifer, E.; Wadepohl, H.; Himmel, H.-J. *Z. Anorg. Allg. Chem.* **2010**, *636*, 543. (p) Zheng, P.; Hong, J.; Liu, R.; Zhang, Z.; Pang, Z.; Weng, L.; Zhou, X. *Organometallics* **2010**, *29*, 1284.

(13) (a) Fu, X.; Tan, C.-H. *Chem. Commun.* **2011**, *47*, 8210. (b) Wild, U.; Kaifer, E.; Himmel, H.-J. *Eur. J. Inorg. Chem.* **2011**, 4220. (c) Li, J.; Liang, W. Y.; Han, K.-L.; He, G. Z.; Li, C. *J. Org. Chem.* **2003**, *68*, 8786. (d) Deutsch, J.; Eckelt, R.; Köckritz, A.; Martin, A. *Tetrahedron* **2009**, *65*, 10365.

(14) *Multiple Bonds between Metal Atoms*, 3rd ed.; Cotton, F. A., Murillo, C. A., Walton, R. A., Eds.; Springer Science and Business Media, Inc.: New York, 2005.

(15) Cotton, F. A.; Dalal, N. S.; Hillard, E. A.; Huang, P.; Murillo, C. A.; Ramsey, C. M. *Inorg. Chem.* **2003**, *42*, 1388.

(16) Cotton, F. A.; Daniels, L. M.; Murillo, C. A.; Timmons, D. J.; Wilkinson, C. C. *J. Am. Chem. Soc.* **2002**, *124*, 9249.

(17) (a) Clérac, R.; Cotton, F. A.; Donahue, J. P.; Murillo, C. A.; Timmons, D. J. *Inorg. Chem.* **2000**, *39*, 2581. (b) Cotton, F. A.; Donahue, J. P.; Gruhn, N. E.; Lichtenberger, D. L.; Murillo, C. A.; Timmons, D. J.; Van Dorn, L. O.; Villagrán, D.; Wang, X. *Inorg. Chem.* **2006**, *45*, 201.

(18) (a) Berry, J. F.; Cotton, F. A.; Huang, P.; Murillo, C. A. *Dalton Trans.* **2003**, 1218. (b) Cotton, F. A.; Dalal, N. S.; Huang, P.; Ibragimov, S. A.; Murillo, C. A.; Piccoli, P. M. B.; Ramsey, C. M.; Schultz, A. J.; Wang, X.; Zhao, Q. *Inorg. Chem.* **2007**, *46*, 1718.

(19) For example, see: (a) Cotton, F. A.; Dalal, N. S.; Huang, P.; Murillo, C. A.; Stowe, A. C.; Wang, X. *Inorg. Chem.* **2003**, *42*, 670. (b) Cotton, F. A.; Chiarella, G. M.; Dalal, N. S.; Murillo, C. A.; Wang, Z.; Young, M. D. *Inorg. Chem.* **2010**, *49*, 319.

(20) Chiarella, G. M.; Cotton, F. A.; Murillo, C. A. *Chem. Commun.* **2011**, *47*, 8940.

(21) Cotton, F. A.; Murillo, C. A.; Timmons, D. J. *Chem. Commun.* **1999**, 1427.

(22) Berry, J. F.; Cotton, F. A.; Huang, P.; Murillo, C. A.; Wang, X. *Dalton Trans.* **2005**, 3713.

(23) Cotton, F. A.; Gu, J.; Murillo, C. A.; Timmons, D. J. *J. Am. Chem. Soc.* **1998**, *120*, 13280.

(24) (a) Cotton, F. A.; Gruhn, N. E.; Gu, J.; Huang, P.; Lichtenberger, D. L.; Murillo, C. A.; Van Dorn, L. O; Wilkinson, C. C. *Science* **2002**, *298*, 1971. (b) Cotton, F. A.; Durivage, J. C.; Gruhn, N. E.; Lichtenberger, D. L.; Murillo, C. A.; Van Dorn, L. O.; Wilkinson, C. C. *J. Chem. Phys. B* **2006**, *110*, 19793.

(25) Chiarella, G. M.; Cotton, F. A.; Durivage, J. C.; Lichtenberger, D. L.; Murillo, C. A. *J. Am. Chem. Soc.* **2013**, *135*, 17889.

(26) Carlson-Day, K. M.; Eglin, J. L.; Smith, L. T.; Staples, R. J. *Inorg. Chem.* **1999**, *38*, 2216.

(27) Cotton, F. A.; Daniels, L. M.; Ren, T. *Inorg. Chem.* **1999**, *38*, 2221.
(28) Note that $W_2(\mu\text{-TMhpp})_4Cl_2$ has been fully characterized. See ref 25.
(29) Cotton, F. A.; Daniels, L. M.; Murillo, C. A.; Slaton, J. G. *J. Am. Chem. Soc.* **2002**, *124*, 2878.
(30) Zurek, J. M.; Paterson, M. J. *Inorg. Chem.* **2009**, *48*, 10652.
(31) Chisholm, M. H.; Cook, C. M.; Folting, K.; Streib, W. E. *Inorg. Chim. Acta* **1992**, *198*−*200*, 63.
(32) Chaudhuri, P.; Wieghardt, K.; Gebert, W.; Jibril, I.; Huttner, G. *Z. Anorg. Allg. Chem.* **1985**, *521*, 23.
(33) Cotton, F. A.; Donahue, J. P.; Hall, M. B.; Murillo, C. A.; Villagrán, D. *Inorg. Chem.* **2004**, *43*, 6954.
(34) Mattes, V. R.; Mennemann, K. *Z. Anorg. Allg. Chem.* **1977**, *437*, 175.
(35) Cotton, F. A.; Murillo, C. A.; Yu, R.; Zhao, Q. *Inorg. Chem.* **2006**, *45*, 9046.
(36) Cotton, F. A.; Li, Z.; Murillo, C. A.; Wang, X.; Yu, R.; Zhao, Q. *Inorg. Chem.* **2007**, *46*, 3245.
(37) Unsurprisingly data for other models in Figure 4 do not support the models for neutral, hypothetical **1**′ or **1H**′. Because **1** has two cations, the only reason those calculations were undertaken was to serve as comparison for the calculations of the ionic forms. Additionally, as shown in Table 2 and Supporting Information, Table S1, both basis sets 1 and 2 gave similar results.
(38) The MOs in Supporting Information, Figure S1 for the $[W(\mu\text{-O})(\mu\text{-TMhpp})Cl_2]_2^{2-}$ anion in **1** show that the metal-based σ and π bonds in HOMO−1 and HOMO are perturbed by the p orbitals from the bridging O^{2-} and axial Cl^- ions. This perturbation is consistent with the high percentage of ligand characters in the HOMO and HOMO−1 orbitals in Supporting Information, Table S3. For additional details see Supporting Information.
(39) An analogous MO interaction diagram between the occupied metal-based orbitals and ligand lone pairs is given in Supporting Information, Figure S4.
(40) For the appropriateness of using NBO on systems containing dimetal units, for example, see: Fang, W. J.; He, Q.; Tan, Z. F.; Liu, C. Y.; Lu, X.; Murillo, C. A. *Chem.—Eur. J.* **2011**, *17*, 10288.
(41) The increase in pressure also allowed an increase in the boiling point of the solvent during the reaction process.
(42) *SMART for Windows NT*, version 5.618; Bruker Advanced X-ray Solutions, Inc.: Madison, WI, 2001.
(43) *SAINT. Data Reduction Software. Version 6.36A*; Bruker Advanced X-ray Solutions, Inc.: Madison, WI. 2001.
(44) *SADABS. Area Detector Absorption and other Corrections Software, Version 2.05*; Bruker Advanced X-ray Solutions, Inc.: Madison. WI, 2001.
(45) Sheldrick, G. M. *SHELXTL, version 6.12*; Bruker Advanced X-ray Solutions, Inc.: Madison, WI, 2002.
(46) For example, see: Cotton, F. A.; Murillo, C. A.; Wang, X.; Wilkinson, C. C. *Inorg. Chim. Acta* **2003**, *351*, 191.
(47) (a) Hohenberg, P.; Kohn, W. *Phys. Rev.* **1964**, *136*, B864. (b) Parr, R. G.; Yang, W. *Density-Functional Theory of Atoms and Molecules;* Oxford University Press: Oxford, 1989.
(48) (a) Becke, A. D. *Phys. Rev. A* **1988**, *38*, 3098. (b) Becke, A. D. *J. Chem. Phys.* **1993**, *98*, 1372. (c) Becke, A. D. *J. Chem. Phys.* **1993**, *98*, 5648.
(49) Lee, C.; Yang, W.; Parr, R. G. *Phys. Rev. B* **1988**, *37*, 785.
(50) Frisch, M. J.; Trucks, G. W.; Schlegel, H. B.; Scuseria, G. E.; Robb, M. A.; Cheeseman, J. R.; Montgomery, J. A., Jr.; Vreven, T.; Kudin, K. N.; Burant, J. C.; Millam, J. M.; Iyengar, S. S.; Tomasi, J.; Barone, V.; Mennucci, B.; Cossi, M.; Scalmani, G.; Rega, N.; Petersson, G. A.; Nakatsuji, H.; Hada, M.; Ehara, M.; Toyota, K.; Fukuda, R.; Hasegawa, J.; Ishida, M.; Nakajima, T.; Honda, Y.; Kitao, O.; Nakai, H.; Klene, M.; Li, X.; Knox, J. E.; Hratchian, H. P.; Cross, J. B.; Bakken, V.; Adamo, C.; Jaramillo, J.; Gomperts, R.; Stratmann, R. E.; Yazyev, O.; Austin, A. J.; Cammi, R.; Pomelli, C.; Ochterski, J. W.; Ayala, P. Y.; Morokuma, K.; Voth, G. A.; Salvador, P.; Dannenberg, J. J.; Zakrzewski, V. G.; Dapprich, S.; Daniels, A. D.; Strain, M. C.; Farkas, O.; Malick, D. K.; Rabuck, A. D.; Raghavachari, K.; Foresman, J. B.; Ortiz, J. V.; Cui, Q.; Baboul, A. G.; Clifford, S.; Cioslowski, J.; Stefanov, B. B.; Liu, G.; Liashenko, A.; Piskorz, P.; Komaromi, I.; Martin, R. L.; Fox, D. J.; Keith, T.; Al-Laham, M. A.; Peng, C. Y.; Nanayakkara, A.; Challacombe, M.; Gill, P. M. W.; Johnson, B.; Chen, W.; Wong, M. W.; Gonzalez, C.; Pople, J. A. *Gaussian 03*, Revision E.01; Gaussian, Inc.: Wallingford, CT, 2004.
(51) (a) Wadt, W. R.; Hay, P. J. *J. Chem. Phys.* **1985**, *82*, 284. (b) Hay, P. J.; Wadt, W. R. *J. Chem. Phys.* **1985**, *82*, 299.
(52) Dunning, T. H.; Hay, P. J. In *Modern Theoretical Chemistry. 3. Methods of Electronic Structure Theory;* Schaefer, H. F., III, Ed.; Plenum Press: New York, 1977; pp 1−28.
(53) (a) Dunning, T. H. *J. Chem. Phys.* **1989**, *90*, 1007. (b) Woon, D. E.; Dunning, T. H. *J. Chem. Phys.* **1993**, *98*, 1358. (c) Wilson, A. K.; Woon, D. E.; Peterson, K. A.; Dunning, T. H. *J. Chem. Phys.* **1999**, *110*, 7667.